Experimental measurement of covariance matrix of two-mode entangled state[†]

YU XuDong, LI Wei, JIN YuanBin & ZHANG Jing[*]

State Key Laboratory of Quantum Optics and Quantum Optics Devices, Institute of Opto-Electronics, Shanxi University, Taiyuan 030006, China

A two-mode entangled state was generated experimentally through mixing two squeezed lights from two optical parametric amplifiers on a 50/50 beam splitter. The entangled beams were measured by means of two pairs of balanced homodyne detection systems respectively. The relative phases between the local beams and the detected beams can be locked by using the optical phase modulation technique. The covariance matrix of the two-mode entangled state was obtained when the relative phase of the local beam and the detected beam in one homodyne detection system is locked and the other is scanned. This method provides a way by which one can extract the covariance matrix of any selected quadrature components of two-mode Gaussian state.

Entangled state is a type of quantum states that can not be decomposed into pure local states of the subsystems, and in which the quantum correlations shared by the subsystems are very stronger than the classical correlations. Entanglement has a critical role in quantum information process, such as quantum teleportation [1,2], quantum dense coding [3–5], entanglement swapping [6–9].

Entanglement detection and characterization always has been a topic of interest for researchers because it is much helpful for understanding the nature of the quantum states, increasing the fidelity and optimizing the quantum communication protocol. The discrete variable states can be described in the finite-dimensional Hilbert space, but it is difficult for the continuous variable (CV) system with infinite dimensions. However for the CV Gaussian entangled state, it can be fully characterized by the covariance matrix. The first experiment of the characterization of the CV entangled state has been performed by Bowen et al. [10] in 2004. In the experiment, they locked all of the phases. Some other research groups have performed the measurement according to the different schemes or setups [11–17], for instance, simultaneously scanning the relative phases of the homodyne detection systems [15], or using a single homodyne detector [16,17]. Herein we present a measurement of the CV Gaussian two-mode entangled state by two pairs of balanced homodyne detection systems, in one of which the relative phase of the local beam and the detected beam is locked and the other is scanned. This scheme can help one to measure the covariance matrix of any selected quadrature components of the two-mode state. The two-mode entangled state is generated through mixing two quadrature squeezed lights from two degenerate optical parametric amplifiers (DOPA) on a 50/50 beam splitter based on our previous experimental setup [18–23]. We modulate the injected optical beams of the two DOPA with two phase modulators respectively. Hence we can obtain the error signal via the relative phase between the

*Corresponding author (email: jzhang74@sxu.edu.cn)

†Contributed by ZHANG Jing (Associate Editor)

local beam and the detected beam and lock the relative phases [23]. Consequently, we can measure the covariance and calculate the covariance matrix.

1 Covariance matrix of bipartite Gaussian state

The output state of the OPA is Gaussian approximately if the Hamiltonian is quadratic [24]. Here we also assume that the transformation (linear or bilinear Hamiltonian [25,26]) in the experiment is the Gaussian operation. Considering the N mode Gaussian states ρ, in the canonical coordinate, $\hat{R} = (\hat{X}_1, \hat{Y}_1, \ldots, \hat{X}_N, \hat{Y}_N)$, the characteristic function is given as

$$\chi_\rho(\xi) = \text{Tr}[\rho W_\xi], \tag{1}$$

where $W_\xi = \exp(i\xi^T R)$ is the Weyl operator. So the characteristic function is

$$\chi_\rho(\xi) = \exp\left(-\frac{1}{4}\xi^T\sigma\xi + iD^T\xi\right), \tag{2}$$

where $\sigma = \sigma^T$ is the covariance matrix (CM), D is the first moment. Thus the Gaussian state can be described by the first and second moment completely. However the first moment can be adjusted arbitrarily through local unitary transformation, and it also doesn't affect the entanglement. Hence we do not consider this herein. Here we just consider the bipartite entangled state. Correspondingly the canonical coordinate $\hat{R} = (\hat{X}_1, \hat{Y}_1, \hat{X}_2, \hat{Y}_2)$, the mode operator $\hat{a}_j$, $j = 1, 2$, and the quadrature operators $\hat{X}_j = \hat{a}_j + \hat{a}_j^\dagger$, $\hat{Y}_j = \frac{1}{i}(\hat{a}_j - \hat{a}_j^\dagger)$. The covariance matrix are positive real symmetric, and can be written as:

$$\sigma = \begin{pmatrix} A & C \\ C^T & B \end{pmatrix}, \tag{3}$$

where A, B, C are the real 2×2 matrix, A and B are the autocorrelation matrices of the single beams. C is the mutual correlation matrix. The element of the matrix σ is

$$\begin{aligned} \sigma_{mn} &= \frac{1}{2}\langle \hat{R}_m\hat{R}_n + \hat{R}_n\hat{R}_m \rangle - \langle \hat{R}_m \rangle\langle \hat{R}_n \rangle \\ &= \frac{1}{2}\langle \delta\hat{R}_m\delta\hat{R}_n + \delta\hat{R}_n\delta\hat{R}_m \rangle, \end{aligned} \tag{4}$$

where $\delta\hat{R}_j = \hat{R}_j - \langle\hat{R}_j\rangle$. According to the Heisenberg inequality, the covariance matrix needs to satisfy [24]

$$\sigma + i\Omega \geq 0, \tag{5}$$

where $\Omega = \bigoplus_{j=1}^{2} \omega$, $\omega = \begin{pmatrix} 0 & 1 \\ -1 & 0 \end{pmatrix}$, Ω is the two-mode symplectic matrix. The covariance matrix can be converted into the standard form through the local symplectic transformation [27,28]

$$S^T\sigma S = \begin{pmatrix} A' & C' \\ C'^T & B' \end{pmatrix} = \begin{pmatrix} a & 0 & c_1 & 0 \\ 0 & a & 0 & c_2 \\ c_1 & 0 & b & 0 \\ 0 & c_2 & 0 & b \end{pmatrix}, \tag{6}$$

where $S = S_1 \bigoplus S_2$, a, b, c_1, c_2 can be determined by the four local symplectic invariants $I_1 = \text{Det}(A) = a^2$, $I_2 = \text{Det}(B) = b^2$, $I_3 = \text{Det}(C) = c_1c_2$ and $I_4 = \text{Det}(\sigma) = (ab - c_1^2)(ab - c_2^2)$. According to eq. (5), we can obtain $I_1 + I_2 + I_3 \leq 4I_4 + 1/4$. The eigenvalues of the symplectic matrix eq. (6) are such that

$$d_\pm = \sqrt{\frac{\Delta \pm \sqrt{\Delta^2 - 4I_4}}{2}}, \tag{7}$$

where $\Delta = I_1 + I_2 + 2I_3$. So the eq. (5) becomes $d_- \geq 1/2$.

2 Experimental setup

Figure 1 shows the experimental setup. The harmonic light (532 nm) from the diode-pumped intracavity frequency-doubled laser (continuous-wave ring Nd:YVO$_4$+KTP) pumped two optical parametric amplifiers. The fundamental light (1064 nm) was separated into three parts. One of which was transmitted through a mode-cleaning cavity and used as the local field of the balanced homodyne detection. The others used as the signal fields were injected into the two OPAs respectively. The relative phases between the pump fields and the signal fields were adjusted by the reflective mirrors mounted on the piezoelectric ceramic transducers (PZTs) before the OPAs. The mode-cleaning cavity and the OPAs were concentric resonators with the lengths of about 60 mm, whose input and output couplers were concave mirrors and had the 30 mm curvature radius. The reflections of the input couplers of the OPA1 and OPA2 were 99.5% at 1064 nm, and the intensity transmissions were 70% and 80% at 532 nm, respectively. The output mirrors of the OPA1 and OPA2 had the power transmissions of 5% and 4% at 1064 nm and the reflections of about 99.5% at 532 nm. The nonlinear media of the optical parametric process were the periodically poled KTP crystals whose tem-
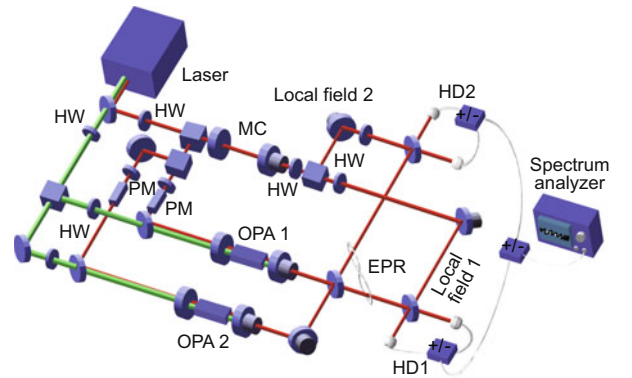
Figure 1 (Color online) Schematic of the experimental setup. OPA: optical parametric amplifiers below threshold to generate the quadrature squeezed states; DBS: Dichroic beam splitter; HW: half wave plate; PBS: polarizing beam splitter; BS: beam splitter; PM: phase modulator; HD1,2: balanced homodyne detection system; PZT: piezoelectric transducer; MC: mode cleaning cavity.

peratures were controlled by the temperature controllers at 36.5°C and 36.9°C for the OPA1 and OPA2. The powers of the signal fields were 15 mW and 10 mW before the OPAs. The pump fields were 86 mW and 83 mW (the thresholds of the OPA1 and OPA2 were 173 mW and 176 mW, respectively), which generated the gain of about 4 for the parametric process when the signal fields were in phase with the pump lights. The powers of two output fields were about 8 μW. They were mixed on a 50/50 beam splitter, the fringe visibility was 97%, and the relative phase was locked at $\pi/2$. Thus the entangled state was generated, that is $\delta^2(\hat{Y}_1 + \hat{Y}_2) \to 0$ and $\delta^2(\hat{X}_1 - \hat{X}_2) \to 0$ under perfect squeezing condition.

3 Experimental results and discussion

The entangled state was measured by two pairs of the balanced homodyne detection systems. The fringe visibilities of the EPRs and the local fields were 95% and 96%, respectively. Figures 2(a) and (b) are the noise spectra of the single EPR beams when the relative phases between the local

fields and the EPRs were scanned. The noise of the quadrature components are different for each EPR beam. The reason is that the output squeezing of the two OPAs are different (the intracavity losses, the gains and the transmissions are different). The maximum and minimum values with $\pi/2$ phase difference in the curves b of Figures 2(a) and (b) are chosen as the quadrature amplitude and phase. Thus the diagonal elements of the autocorrelation block matrices are $\sigma_{11} = \delta^2\hat{X}_1 = 3.0$, $\sigma_{22} = \delta^2\hat{Y}_1 = 2.2$, $\sigma_{33} = \delta^2\hat{X}_2 = 3.1$, $\sigma_{44} = \delta^2\hat{Y}_2 = 2.1$. Because there is no crosstalking between the quadrature components, the off diagonal elements of the autocorrelation block matrices are all 0, i.e., $\sigma_{12} = \sigma_{21} = \sigma_{34} = \sigma_{43} = 0$.

In order to identify and lock the relative phases between the local fields and the EPR beams, the signal fields pass through the phase modulators before the two OPAs. The modulation radio-frequencies (RF) are 3.8 MHz and 3.6 MHz, respectively. The mixed signals of the electronic signals of the balanced homodyne detectors and the local signals (the RF modulation signals) are used as the error signals of
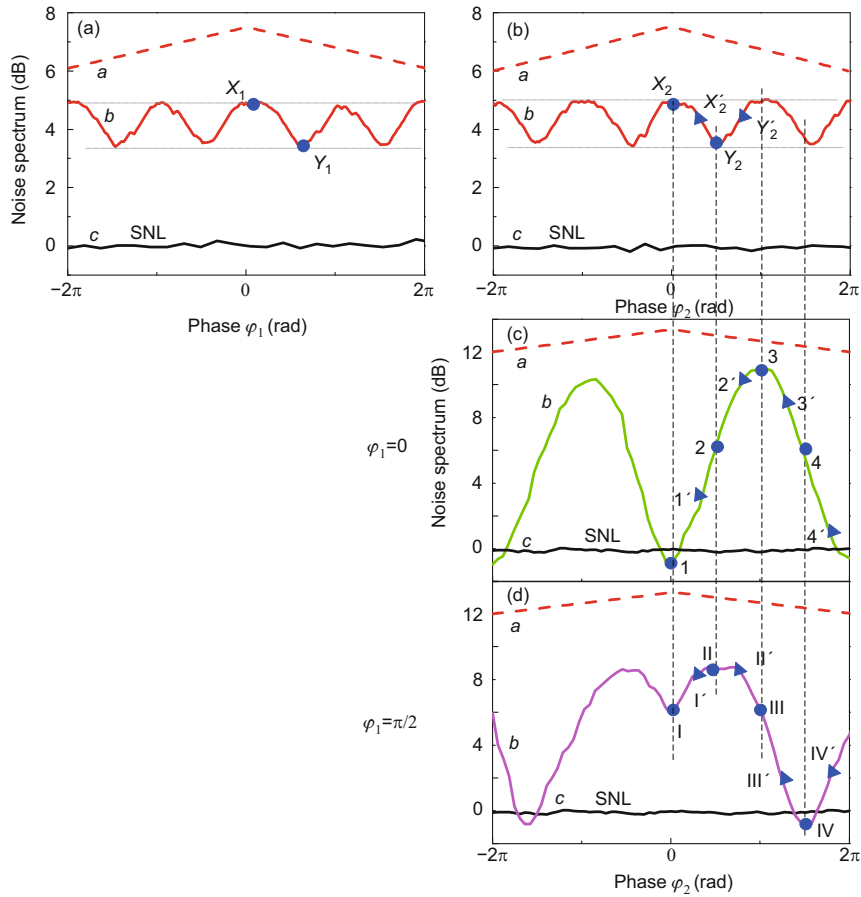
Figure 2 Noise power spectra of the EPR entangled state. The quadrature spectra are measured at the sideband frequency of 5 MHz, RBW 300 kHz, VBW 300 Hz. Panel (a) and (b) show the noise power spectra of each of EPR beams. Red dashed lines are the scanning voltage on the PZTs on the local beams. Red lines are noise power spectra of the single EPRs. Black lines are the SNL. (c) and (d) the correlated spectra of the EPR beams. Red dashed lines are the scanning voltage on the PZT on the local beam2. Green line of (c) is noise spectrum in the correlation measurement when the relative phase of the local beam1 and the EPR1 is locked at 0 and the other is scanned. Pink line of (d) is noise spectrum in the correlation measurement when the relative phase of the local beam1 and the EPR1 is locked at $\pi/2$ and the other is scanned.

the PID locking circuits. The relative phases can be locked at 0 or $\pi/2$ by exchanging the local signals of the mixers. Figures 2(c) and (d) show the measurement when the relative phases between the local beam1 and the EPR1 is locked at 0 or $\pi/2$ and the other is scanned. Consequently we can measure $\delta^2(\hat{X}_1 \pm \hat{X}_2)$ from points 1 and 3 and $\delta^2(\hat{Y}_1 \pm \hat{Y}_2)$ from points II and IV. The noise spectrum of the sum of the quadrature phases is lower 1.3 dB than the SNL, i.e., $\delta^2(\hat{Y}_1 + \hat{Y}_2) = 0.74$. The noise spectrum of the difference of the quadrature amplitudes is lower 1.1 dB than the quantum shot noise limit, i.e., $\delta^2(\hat{X}_1 - \hat{X}_2) = 0.78$. The corresponding canonical conjugate quantities are $\delta^2(\hat{Y}_1 - \hat{Y}_2) = 8.7$, $\delta^2(\hat{X}_1 + \hat{X}_2) = 11.6$. Expanding the covariance

$$\delta^2(\hat{X}_1 \pm \hat{X}_2) = \delta^2\hat{X}_1 + \Delta^2\hat{X}_2 \pm 2\sigma_{13(31)},$$
$$\delta^2(\hat{Y}_1 \pm \hat{Y}_2) = \delta^2\hat{Y}_1 + \delta^2\hat{Y}_2 \pm 2\sigma_{24(42)}, \quad (8)$$

we can get the diagonal elements of the mutual correlation matrix. The off-diagonal terms of the mutual correlation matrix can be extracted according to the points 2 and 4 in Figure 2(c) and the points I and III in Figure 2(d), which are $\delta^2(\hat{X}_1 - \hat{Y}_2) = 5.5$, $\delta^2(\hat{X}_1 + \hat{Y}_2) = 5.0$, $\delta^2(\hat{Y}_1 - \hat{X}_2) = 5.7$ and $\delta^2(\hat{Y}_1 + \hat{X}_2) = 5.6$. Thus the off-diagonal terms can be calculated according to the formulas as thus

$$\delta^2(\hat{X}_1 \pm \hat{Y}_2) = \delta^2\hat{X}_1 + \Delta^2\hat{Y}_2 \pm 2\sigma_{14(41)},$$
$$\delta^2(\hat{Y}_1 \pm \hat{X}_2) = \delta^2\hat{Y}_1 + \delta^2\hat{X}_2 \pm 2\sigma_{23(32)}. \quad (9)$$

Then the covariance matrix of the EPR beams can be given as:

$$\sigma = \begin{pmatrix} 3.0 & 0 & 2.7 & 0 \\ 0 & 2.2 & -0.1 & -1.8 \\ 2.7 & -0.1 & 3.1 & 0 \\ 0 & -1.8 & 0 & 2.1 \end{pmatrix}. \quad (10)$$

Although the values of the covariance matrix are close with our expectation, the error still exist because of the phase drift of the relative phase of the local beam2 and EPR2 in the balanced homodyne detection system2 during the measurement.

This measurement also provides a method which can help us to extract the covariance matrix of any quadrature components. In Figures 2(c) and (d), we fix the the relative phase of the local beam 1 and the EPR1 at 0 (Figure 2(c)) and $\pi/2$ (Figure 2(d)) respectively, and scan the the relative phase of the local beam 2 and the EPR2. Here, the selected quadrature components of the EPR1 are the same as the above discussion with $\delta\hat{X}'_1 = \delta\hat{X}_1$ and $\delta\hat{Y}'_1 = \delta\hat{Y}_1$, and the quadrature components for the EPR2 are arbitrary. They can be defined as $\delta\hat{X}'_2 = \delta\hat{X}_2 \cos(\theta_2) + \delta\hat{Y}_2 \sin(\theta_2)$ and $\delta\hat{Y}'_2 = \delta\hat{X}_2 \cos(\theta_2 + \pi/2) + \delta\hat{Y}_2 \sin(\theta_2 + \pi/2)$, this is, the canonical coordinate in the measurement is rotated, which corresponds to an unitary transformation. Here we chose $\theta_2 = 55.4°$ and extract the CM. The terms of the autocorrelation matrix A are given as discussed above. The diagonal terms of the autocorrelation matrix of EPR2 can be easily obtained according to Figure 2(b) (the blue triangle points), $\sigma'_{33} = \delta^2\hat{X}'_2 = 2.6$, $\sigma'_{44} = \delta^2\hat{Y}'_2 = 2.9$. However the off-diagonal elements of the autocorrelation matrix B are not 0,

and which can not be measured directly because of the uncertainty relation. However these terms can be calculated according to the relationship

$$\sigma'_{34} = \sigma'_{43} = \delta\hat{X}'_2\delta\hat{Y}'_2 = [\delta\hat{X}_2 \cos(\theta_2) + \delta\hat{Y}_2 \sin(\theta_2)]$$
$$\times \left[\delta\hat{X}_2 \cos\left(\theta_2 + \frac{\pi}{2}\right) + \delta\hat{Y}_2 \sin\left(\theta_2 + \frac{\pi}{2}\right)\right] = 0.1. \quad (11)$$

The diagonal elements of the mutual matrix can be extracted from the points 1′ and 3′ in Figure 2(c) and the points II′ and IV′ in Figure 2(d). Then we obtain $\sigma'_{13,31} = 1.4$ and $\sigma'_{24,42} = -1.4$. Here the off-diagonal terms of the mutual matrix are not 0 because of the correlations of the quadrature components, but which can be determined according to the points 2′ and 4′ in Figure 2(c) and points I′ and III′ in Figure 2(d). Similarly, we obtain $\sigma'_{14,41} = -2.4$ and $\sigma'_{23,32} = -1.4$. So the CM of the selected quadrature components is

$$\sigma' = \begin{pmatrix} 3.0 & 0 & 1.4 & -2.4 \\ 0 & 2.2 & -1.4 & -1.4 \\ 1.4 & -1.4 & 2.6 & 0.1 \\ -2.4 & -1.4 & 0.1 & 2.9 \end{pmatrix}. \quad (12)$$

On the other hand, the CM in eq. (12) can be obtained from CM in eq. (10) by the unitary transformation. In the phase space, the unitary transformation can be defined as:

$$S^\dagger R S = MR + D', \quad (13)$$

where S is the unitary operator, D' is the rotated first moment, and M is the corresponding symplectic matrix

$$M = \begin{pmatrix} \cos(\theta_1) & \sin(\theta_1) & 0 & 0 \\ -\sin(\theta_1) & \cos(\theta_1) & 0 & 0 \\ 0 & 0 & \cos(\theta_2) & \sin(\theta_2) \\ 0 & 0 & -\sin(\theta_2) & \cos(\theta_2) \end{pmatrix}, \quad (14)$$

where $\theta_1 = 0$ and $\theta_2 = 55.4°$. Consequently, the characteristic function of the state in the new canonical coordinate is

$$\text{Tr}[S^\dagger \rho S W(\xi)] = \text{Tr}[\rho\exp[i\xi^\text{T} S^\dagger R S]]$$
$$= \exp\left[-\frac{1}{4}\xi^\text{T}\sigma'\xi + i\xi^\text{T}\tilde{D}\right], \quad (15)$$

where $\sigma' = M\sigma M^\text{T}$, $\tilde{D} = MD + D'$. Thus we can calculate the CM directly from eq. (10) according to the symplectic transformation

$$\sigma'_T = M\sigma M^\text{T} = \begin{pmatrix} 3.0 & 0 & 1.5 & -2.2 \\ 0 & 2.2 & -1.5 & -1.0 \\ 1.5 & -1.5 & 2.4 & -0.5 \\ -2.2 & -1.0 & -0.5 & 2.8 \end{pmatrix}. \quad (16)$$

Comparing CM in eq. (16) with that in eq. (12), σ' and σ'_T are close with our expectation.

The relative phase of the local beam and the detected beam in homodyne detection system 1 is locked at 0 or $\pi/2$ in the experiment. In reality, the relative phase can be locked at any angle value because the offset of the PID circuit can be adjusted in a certain range and the local signal of the mixer of the relative phase locking system can also be exchanged. Hence the covariance matrix of any selected quadrature components can be extracted according to this scheme.

4 Conclusion

Herein we experimentally generate two-mode CV entangled state, and measure the covariance matrix of the entangled state by using two balanced homodyne detection systems. The relative phase of the local beams and the detected beams can be locked through the optical phase modulation technique. The detection system in this work can be used to measure the covariance matrix of the arbitrary selected quadrature components of the two EPRs. This work will help us obtain all information of two-mode entangled states for optimizing the quantum communication in the future experiments. Herein we did not report non-Gaussian character of generating EPR entangled state. Detecting and Quantifying non-Gaussianity [29] will be investigated in detail in the future.

1 Bouwmeester D, Pan J W, Mattle K, et al. Experimental quantum teleportation. Nature, 1997, 390: 575–579

2 Furusawa A, Sørensen J L, Braunstein S L, et al. Unconditional quantum teleportation. Sciene, 1998, 282: 706–709

3 Mattle K, Weinfurter H, Kwiat P G, et al. Dense coding in experimental quantum communication. Phys Rev Lett, 1996, 76: 4656–4659

4 Li X Y, Pan Q, Jing J T, et al. Quantum dense coding exploiting a bright Einstein-Podolsky-Rosen beam. Phys Rev Lett, 2002, 88: 047904

5 Jing J T, Zhang J, Yan Y, et al. Experimental demonstration of tripartite entanglement and controlled dense coding for continuous variables. Phys Rev Lett, 2003, 90: 167903

6 Pan J W, Bouwmeester D, Weinfurter H, et al. Experimental entanglement swapping: Entangling photons that never interacted. Phys Rev Lett, 1998, 80: 3891–3894

7 Jia X J, Su X L, Pan Q, et al. Experimental demonstration of unconditional entanglement swapping for continuous variables. Phys Rev Lett, 2004, 93: 250503

8 Takei N, Yonezawa H, Aoki T, et al. High-fidelity teleportation beyond the no-cloning limit and entanglement swapping for continuous variables. Phys Rev Lett, 2005, 94: 220502

9 Xie C D, Jia X J, Su X L, et al. Unconditional entanglement swapping of continuous variables—quantum teleportation of entangled state (in Chinese). Physics, 2005, 34: 573–577

10 Bowen W P, Schnabel R, Lam P K, et al. Experimental characterization of continuous-variable entanglement. Phys Rev A, 2004, 69: 012304

11 Patrón G R, Fiurášek J, Cerf N J, et al. Proposal for a loophole-free bell test using homodyne detection. Phys Rev Lett, 2004, 93: 130409

12 Wenger J, Ourjoumtsev A, Brouri T R, et al. Time-resolved homodyne characterization of individual quadrature-entangled pulses. Eur Phys J D, 2004, 32: 391–396

13 DiGuglielmo J, Hage B, Franzen A, et al. Experimental characterization of Gaussian quantum-communication channels. Phys Rev A, 2007, 73: 012323

14 Rigolin G, Oliveira M C D. Complete state reconstruction of a two-mode Gaussian state via local operations and classical communication. Phys Rev A, 2007, 79: 030302

15 Laurat J, Coudreau T, Keller G, et al. Effects of mode coupling on the generation of quadrature Einstein-Podolsky-Rosen entanglement in a type-II optical parametric oscillator below threshold. Phys Rev A, 2005, 71: 022313

16 Auria V D, Porzio A, Solimeno S, et al. Characterization of bipartite states using a single homodyne detector. J Opt B-Quantum Semiclass Opt, 2005, 7: S750

17 Auria V D, Fornaro S, Porzio A, et al. Full characterization of Gaussian bipartite entangled states by a single homodyne detector. Phys Rev Lett, 2009, 102: 020502

18 Ma H L, Wei D, Ye C G, et al. Bright amplitude-squeezed light generation by an optical parametric deamplifier in a periodically poled KTiOPO4 crystal (in Chinese). Acta Phys Sin, 2005, 54: 3637–3640

19 Ye C G, Zhang J. Generation of squeezed vacuum states by PPKTP crystal and its Wigner quasi-probability distribution function reconstruction (in Chinese). Acta Phys Sin, 2008, 57: 6962–6967

20 Di K, Yu X D, Zhang J. Experimental investigation of small-sized squeezed vacuum light device (in Chinese). Acta Sin Quant Opt Sin, 2011, 16: 241–246

21 Zhang J, Ye C G, Gao F, et al. Phase-sensitive manipulations of squeezed vacuum field in an optical parametric amplifier inside an optical cavity. Phys Rev Lett, 2008, 101: 233602

22 Di K, Xie C D, Zhang J. Coupled-resonator-induced transparency with a squeezed vacuum. Phys Rev Lett, 2011, 106: 153602

23 Zhang Y, Yu X D, Di K, et al. Locking the phase of balanced homodyne detection system for squeezed light (in Chinese). Acta Phys Sin, 2013, 62: 084204

24 Simon R, Mukunda N, Dutta B. Quantum-noise matrix for multimode systems: U(n) invariance, squeezing, and normal forms. Phys Rev A, 1994, 49: 1567

25 Olivares S. Quantum optics in the phase space a tutorial on Gaussian states. Eur Phys J Spec Top, 2012, 203: 3

26 Marian P, Marian T A. Squeezed states with thermal noise. I. Photon-number statistics. Phys Rev A, 1993, 47: 4474

27 Simon R. Separability criterion for continuous variable systems. Phys Rev Lett, 2000, 84: 2726–2729

28 Duan L M, Giedke G, Cirac J I, et al. Inseparability criterion for continuous variable systems. Phys Rev Lett, 2000, 84: 2722–2725

29 Genoni M G, Paris M G A. Quantifying non-Gaussianity for quantum information. arXiv:1008.4243